Recrystallization Behaviour of Hot Rolled Aluminium 3004 Alloy

FUI TONG LEE - Alcan International Limited, Kingston Research and Development Center, P.O. Box 8400, Kingston, Ontario K7L 5L9, Canada

Abstract

The development of microstructure, crystallographic texture, hardness and electrical conductivity with recrystallization behaviour of hot rolled aluminium 3004 alloy has been investigated. The work was undertaken so as to better understand and as it is in the control of earing in can stock. Surface shear bands and recovery occurred after hot rolling. After annealing for one hour, recrystallized surface layer with a cube texture and an unrecrystallized core with a rolling texture has been observed for sample with sufficient internal strain energy. The thickness of the recrystallized layer varied from almost zero to almost the full sheet thickness, increasing with warm rolling reduction and annealing time. A good correlation has been found to exist between the amount of recrystallization texture and the driving force for recrystallization. In addition, a general agreement between hardness measurement and microstructure was obtained, recrystallization resulting for the large decrease in hardness and deformation raising the hardness.

Riassunto

L'Autore ha studiato lo sviluppo della microstruttura, della tessitura cristallografica, della durezza e della conduttività elettrica nel corso della ricristallizzazione della lega di alluminio 3004 laminata a caldo. Il lavoro è stato avviato allo scopo di capire meglio e controllare la formazione di difetti superficiali. In seguito a laminazione a caldo si sono prodotte bande trasversali e riassestamento strutturale. Dopo un'ora di riscaldamento si è osservato uno strato superficiale ricristallizzato con struttura cubica ed un nucleo non ricristallizzato con tessitura di laminazione per campioni con sufficiente energia interna di deformazione. Lo spessore dello strato ricristallizzato variava da zero circa a quasi l'intero spessore della lastra, aumentando con la riduzione di laminazione a caldo ed il tempo di riscaldamento. È stata rilevata una buona correlazione tra il quantitativo di struttura di ricristallizzazione e la forza trainante di ricristallizzazione. Si è inoltre ottenuto un generale accordo tra valori di durezza e modificazioni strutturali, osservando che la ricristallizzazione provoca una rilevante diminuzione della durezza, che viceversa aumenta con l'entità della deformazione.

Introduction

Over the past decades, with the general increase in the size of aluminium sheet ingot used for rolling and with more powerful hot mills, the tendency has been for higher temperature to be retained during rolling and for larger reduction to be taken. There is, therefore, despite the stronger recovery effect in aluminium, a greater chance that recrystallization will occur during rolling. Because of the effects of structural changes during fabrication on the properties of the final sheet, it is important to identify under what circumstances recrystallization occurs and to what extent and at what stage in the fabrication cycle.

The experimental technique employed in this investigation was to roll wedge-shaped ingots at various temperature (250 °C-350 °C) in a single pass so as to produce a rolled slab which had undergone reductions, varying between 40% and 60% deformation. The rolled slabs could be quenched after predetermined delay times.

The purpose of this paper is to describe the changes in hardness, microstructure, recrystallization texture and conductivity which occur when aluminium 3004 alloy is annealed at various temperature during warm rolling. With the information obtained, appropriate changes will be made in the processing of 3004 can stock to achieve higher strength without losing control of the tendency to form ears during deep drawing.

Experimental

Material and Sample Preparation

The chemical composition of the aluminium 3004 alloy used in this investigation had a composition of 1.06 wt % Mn, 0.42 wt % Fe, 0.30 wt % Si, 0.22 wt % Cu, 1.02 wt % Mg and 0.02 wt % Cr, balance aluminium. The samples were prepared in the form of wedge-shaped ingots, with the average dimensions of 1.83 cm thick, 3.5 cm width and 11.5 cm in length.

The wedge-shaped samples were given 40%, 50% and 60% reductions at various temperatures of 250, 280, 300 and 350 °C in a single pass, using a laboratory warm rolling mill. The rolled slab was water quenched 15 seconds after exit from mill. Samples were then taken from the wedge-shaped slab after hot

rolling. Samples obtained from each wedge-shaped rolled slab were socked at the rolling temperature in a bath of molten $NaNO_3$ salt for 10, 20, 40 and 60 minutes and quenched respectively. These conditions were chosen to investigate the effect of rolling temperature and annealing time that are encountered in the actual fabrication process. A temperature controller was used to maintain a constant-temperature salt baths to within ± 5 °C.

Optical Microscopy, Hardness and Conductivity Measurements

The extent of recrystallization was determined metallographically for all the samples using the Zeiss microscope. The samples were mounted, polished and anodised in Barker's solution for 60 to 80 seconds to reveal the grain structure. The degree of recrystallization was estimated and recorded using crossed polarize light. The fractional depth of recrystallization is calculated by using the formula below:

$$\text{Fractional depth of recrystallization} = \frac{2 \times \text{Depth recrystallized}}{\text{Specimen thickness}}$$

The recrystallization behaviour was followed by making Vickers micro-hardness measurements before and after annealing treatments. Six diamond impressions were made for each determination using a load of 2 kg at the specimen surface and centre respectively. The temperature needed to achieve 50 pct recrystallization can be determined from microscopy and hardness measurement.

A Fischer Sigmascope tester was used at 15 °C to measure the electrical conductivity for all the surface and centre samples. Conductivity is a measure of the amount of manganese in solution but it also depends on the distribution of other alloying elements, the degree of hot work and other factors to some extent.

Texture Measurements

Texture specimens about 30 mm diameter and 3.6 mm in thickness were prepared for as-hot rolled and annealed samples (e.g. at approximately the centre of the strip thickness and the surface). The sample is ground to the appropriate thickness and surface finish with 400, 600 and 1200 grit papers. After etching for about 10 minutes in 20% caustic soda, the sample was then mounted in the X-ray specimen holder.

The quick texture determination method was used in most cases. It is useful for samples with a significant cube texture component only. The cube texture intensity was calculated from the strength of the (200) Bragg X-ray reflection normal to the sheet surface (i.e. at $\alpha = 90$ °C). This angle corresponds to the centre of the pole figure, where there is a cube texture intensity peak.

The intensities are reported relative to the intensity for a powder sample (random texture). Three measurements were made for each sample, one at the surface and the second at a depth of about half the thickness of the specimen. The cube texture and rolling texture intensities can be inferred because a stronger cube texture corresponds to a weaker rolling texture component and vice versa.

Results

Optical Microscopy

Figure 1 shows the effect of annealing time on the fractional depth of recrystallization for samples given 40%, 50% and 60% hot-rolled reduction in a single pass. No recrystallized grains were observed in the specimens quenched in the first 15 seconds after exit from the mill, however it was expected that dynamic recovery resulted in the formation of subgrain structure and hence softening. The degree of recrystallization observed for samples annealed at low warm rolling temperature (<300 °C) and low pct deformation was generally very low and concentrated near the surface.

For a given rolling reduction, the fractional depth of recrystallization increases with annealing time, but the rate of recrystallization decreases beyond 20 min for samples annealed at 350 °C. Specimens annealed at higher warm rolling temperature and pct rolling reduction are also observed to recrystallize quicker than others. According to the assessment for the driving force (i.e. reciprocal of the time taken for the specimen to 50% recrystallized) clearly, it can be seen that the driving force for recrystallization increases with higher rolling reduction and temperature. That is, the recrystallization rate which is related to the driving force increases with increasing temperature and pct reduction due to the increased atomic mobility.

Figure 2 shows typical microstructures of samples exit from the warm mill. The structure consists entirely of unrecrystallized grains both at centre and surface. The large mass of the mill with respect to that of the samples resulted in a significant temperature drop during deformation. It is expected that the exit temperature obtained in this experiment will be below the critical temperature for recrystallization to occur since it was established that the degree of recrystallization occurring is largely a function of the exit temperature.

Figures 3, 4 and 5 show the typical range of microstructures observed after the annealing of samples warm rolled to 40% and 60% rolling reduction. Figure 3 shows heavily worked grains at the centre of the sample. However, recrystallized grains were readily observed at higher rolling reductions (Figure 4). Similarly comparing Figures 4 and 5, increasing the annealing temperature also increases the depth of recrystallization. Clearly, this is due to the extra strain energy available to overcome the recrystallization threshold to enable nucleation and grain growth during recrystallization.

In figures 4 and 5, recrystallized grains were observed to advance towards the centre as the annealing time increased. The structure consisted of a recrystallized surface layer, a very thin layer of partial recrystallization and the remainder of the thickness in a heavily worked condition. In the recrystallized layer, the grain size at the surface was fine (<5 μm) and became coarser at greater depth, thus indicating more rolling deformation at the surface. At a given pct deformation, the grain size also incraesed with temperature. The grains were pancake-shaped or elongated when studied in the longitudinal section perpendicular to the rolling plane. Shear bands were observed at higher magnification in the elongated grains and they appear to be more marked with increasing pct rolling reduction. The aspect ratio of the grain appears to decreases with increasing annealing temperature and time and at sample surface where the driving force for recrystallization is greatest.

It was also shown that the surface layers recrystallised more easily than the central zone. This difference was ascribed partly to the greater deformation at the surface, which gives it a lower recrystallization temperature and partly to the greater temperature rise at the surface. Annealing for one hour, traces of cold work were observed in the central regions eventhough the surface layers had recrystallised, so the specimen had a markedly cored structure.

Microstructure Changes For Intermetallic Particles

Figure 6 shows typical examples of the microstructures obtained for the distribution of intermetallic particles in the hot rolled and annealed plate (e.g. 60 min given 60% reduction at 350 °C). The distribution of the precipitates was inhomogeneous. In addition, the coarse primary constituents were rolled out into stringers as shown in the long transverse sections indicating that these particles are softer and more ductile than the matrix. Accordingly the distribution of the secondary particles was also elongated in the rolling direction showing regions with no or very few precipitates near the primary particles. These primary and secondary precipitates were assumed to contribute partly for the increase in conductivity during annealing.

Referring to the hardness differences and microstructures observed, it seems that the high hardness of this alloy must be partly attributed to the fine, densely concentrated precipitates. Comparing the hardness value with metallography, the following points were apparent.

1) Surface sample that contains a higher density of fine intermetallic particles showed higher hardness value than the centre,

2) Similarly, surface samples with a large volume of coarse intermetallic and a lower density of fine secondary particles will show a lower hardness value than the centre,

3) Where the density of the intermetallic phases are distributed evenly, then they will show similar hardness.

Inspection of micrographs (e.g. Fig. 6) show that the coarse primary particles has developed in an area which is strongly depleted of precipitates. Nucleation of recrystallization is likely to occur in this precipitate free zone, followed by growth into the surrounding stabilized matrix.

Hardness Measurements

The results of the hardness measurements on the samples at 40%, 50% and 60% warm rolling reductions are shown in Figure 7. Each point represents an average of more than 15 measurements. It shows the general trend to a decrease in hardness at higher rolling temperatures. It appears that higher hot rolling temperatures favour recovery and recrystallization during or immediately after hot rolling. Strain hardening decreases progressively as the working temperature is raised until a temperature is reached above which no effective hardening occurs due to dynamic recovery and recrystallization.

In general, the presence of manganese in solid solution also has a significant effect in the hardness value obtained. Higher working temperatures will probable decreases the concentration of Mn in solution, thus decreases its hardness. Increasing the rolling reduction for any given temperature also increases hardness, due to the higher retained density of dislocations. This increases in hardness continue to occur up to 50% warm rolling reduction beyond which the hardness decreases. Figure 7 also shows that centre samples have lower hardness than the corresponding surface samples. The higher hardness at surface resulted from the inhomogenity of rolling deformation and higher density of fine, densely particles than at the corresponding centre sample.

Typical examples of the hardness measurements plotted against the annealing time for 40%, 50% and 60% warm rolling reductions are shown in Figures 8 and 9. The hardness curves are in gneeral agreement with the microstructures shown earlier, recovery and recrystallization resulting in a low hardness and deformation raising the hardness. Under the conditions in which no primary recrystallization has occurred then the resulting hardness-time-curve shows a continuous gentle descent.

The Mn in solution in this alloy may increase the hardness. Annealing will results in the recovery and recrystallization together with precipitation of Mn from solid solution in the form of intermetallic phases, contributing to the decrease in hardness. The process of recovery was seen to be a significant features of all the curves.

The samples generally show low core hardness (Figure 8) due to the inhomogeneity of the rolling deformation, and a low surface hardness (Figure 9) if partial recrystallization has occurred. Complete softening of the surface specimen for 60% rolling reduction was found to occur at 350 °C soaked for 20 min and this has a hardness value of about 49 HV. Hardness measurement and microstructure observation during annealing also revealed that recrystallization accounts for most of the decrease in hardness.

Crystallographic Texture

Results of the cube texture intensity measurements are shown in Figure 10 where an average of 36 intensities has been taken over the intensities for all samples in similar initial conditions and at near sheet surface and mid-plane of the as-hot rolled and annealed samples. The figure shows that the cube texture intensity increases as the temperature increases. Further, increasing the annealing time for any given temperature also increases the cube texture intensity made on the surface specimen for all rolling reductions. In contrast to surface texture, the effect of cube texture intensity in the centre of specimen with respect to the annealing time was found to be negligible over the temperature range of 250 °C to 350 °C investigated as shown in the figure for all reduction per pass.

The figure also shows that the experimental data plotted for each annealing time can be corrected into an approximate straight line relationship between cube texture intensity and temperature and in the case of surface measurements, approximated parallel straight line relation was obtained but this may not be significant compared with the measurement and sampling errors. It should also be noted that surface samples have higher cube texture intensity than centre samples. The reason for this appears to be due to the faster recovery and recrystallization that has taken place at the surface.

The presence of rolling texture component in the centre samples have resulted in lower cube texture intensity. As seen in the figures, it was also observed that there is no systematic variation of texture intensity for the centre samples in the annealing time and temperature used in this investigation.

Comparing between 40% and 50% rolling reductions of the relative cube texture intensity obtained for near-sheet surface measurement (figure 10 (a-b)), it can be seen that at a given annealing time, the cube texture intensity increases with higher reduction per pass. This is expected since the driving force for recrystallization increases as the hot rolling reduction increases provided the rolling temperature employed does not exceed the critical temperature for rapid recovery. It is expected that strain hardening diminishes at elevated temperatures because of softening via thermally activated recovery.

The recrystallization texture was also found to contain a cube texture component {001}<100>, rolling texture components (for example, {110}<001>, {110}<112>, {123}<634> and {112}<111>) and other components distributed randomly in the Euler space. This cube component {001}<100> increases while the rolling texture component decreases with increasing annealing time.

Conductivity Change in Hot Rolled and Annealed Specimens

The results of surface and centre conductivity measurements of the as-hot rolled and annealed samples given 40%, 50% and 60% warm rolling reductions are shown in Figure 11. The figure shows that conductivity generally increases as the annealing time is extended. The result is partly due to the manganese retained in the solid solution that is precipitated out from the matrix during the annealing period. It should be noted that part of the conductivity change during the annealing process are due to recrystallization, the degree of hot work and the distribution of other alloying elements. The figure also shows that for a given annealing time and temperature, conductivity increases as the rolling reduction in a single pass increases. The higher rolling reduction appears to increase the manganese precipitation from the matrix due to the available of extra stored energy.

It is known that the reduction of dislocation density are also responsible for a decrease in conductivity and hence the rate of conductivity change decreased rapidly during the early stage of annealing as recovery occurs rapidly (e.g. compare figures 8 & 9 for surface measurements). However, the change in conductivity for the centre samples are generally very low compared with surface measurement.

Discussion

The results of this investigation show that the amount of recrystallization texture can be correlated to

the driving force for recrystallization. At higher rolling reduction, the density of dislocations generated and hence the amount of strain hardening will be larger, consequently increasing its hardness. Although all as-hot rolled samples examined show no sign of recrystallization but partial recovery process have occurred and shear bands were observed in the microstructure. These shear bands are caused by the heavy deformation process and they appear to be more marked with increasing rolling reduction.

The degree of recovery and recrystallization occurring increases with the exit mill tempeature. The exit temperature obtained in this investigation may be below the critical temperature for recrystallization to occurr which apparently resulted in insufficient driving force for recrystallization nucleation but is sufficient to increase atomic mobility to cause recovery. In addition, at smaller amount of reductions and rolling temperature, the driving force for recrystallization is reduced such that the dwell time of 15 seconds is insufficient for recrystallization to start. Therefore for a significant amount of recrystallization to occur throughout the rolled samples, larger pct deformation and the dwell time at the higher rolling temperature used in the processing route should be increased, that is, to allow enough time for recrystallization to occur.

With an unrecrystallized structure after hot working, the recrystallization texture can be modified by adjusting annealing parameters such as soak temperature and time. In this regard, for a given annealing time, recrystallization will occur provided the rolling reduction reached a critical value. When this critical value is reached, the internal strain energy generated by the increased deformation will provide the driving force to overcome the recrystallization threshold to enable nucleation grain growth to occur. This energy stored in the structure is the driving force for recovery and recrystallization. The driving force is usually given by the decrease in free energy due to the elimination of lattice defects by boundary migration. The lattice defects being eliminated [1] are dislocations of the worked structure, dislocation networks (i.e. subgrain boundaries) of a recovered structure and grain boundaries. The driving force F for boundary migration can be approximated by [1, 2]:

$$F = \frac{1}{2} Gb^2 \varrho$$

where G is the shear modulus, b the Burgers vector, and ϱ the dislocation density. Therefore the driving force increases when the degree of deformation is increased assuming ϱ is increased. However, during the recovery process, part of the driving force F is lost, due to annihilation of dislocations. The aluminium alloy used in this investigation shows a marked preference for recovery during hot working in agreement with the hardness measurement (Figure 7).

It was also shown that the amount of recrystallization decreases from the surface inwards towards the centre of all the sample and that recrystallized grains tend to be finer nearer the surface but coarser recrystallized grains below the outer surfaces (Figure 5). One explanation for this is that the working processes are such that deformation is more severe at the outer surface than toward the centre of the sample. Thus, an effective strain hardening gradient is generated in the through thickness direction of the resulting microstructure perpendicular to the rolling plane at the completion of working. This effective strain hardening straddle the critical strain required to produce recrystallization under a given combination of time and temperature. Holding at the temperature after hot working or subsequent reheating can produce recrystallization in the surface region that exceeds the critical strain. Hence larger recrystallized grains are observed under such conditions. The greater deformation at the outer sample surface will also increases the driving force for recovery and recrystallization, resulting in the surface layers recrystallized more easily than towards the central zone.

It should also be remarked that some samples examined show low core hardness due to inhomogeneity of rolling deformation and lower density of fine, densely secondary particles and low surface hardness if recovery and recrystallization have occurred.

In the hot rolled samples examined the strength of the cube recrystallization texture depends on the rolling and annealing temperature, and the extent of deformation. It was seen that the cube texture intensity increases with higher rolling temperature and reduction per pass. This is expected because

during hot deformation, the distortions in the lattice are removed by recovery and partial recrystallization. As expected, the increase in this cube texture intensity will lead to a decrease in rolling texture component. These results were also demonstrated by a decrease in hardness with higher rolling temperature and smaller reduction (Figure 7). At higher rolling temperatures, recovery is rapid and so the texture remains relatively random and it is expected that the greater propensity for recovery also ensures that slip systems initially operative are not appreciably hardened and therefore this results in low hardness.

It should be pointed out that recrystallization does not always resulted in cube texture but can lead to a retained rolling texture or a mixture of texture component (random texture) depending on the recovery and recrystallization condition. This was probably partly the reason for some scattered points in the plot relating cube texture and temperature. Although recrystallization in hot rolling is an important factor influencing texture, it is by no means the only hot rolling parameter of the hot rolled structure which can have an influence. Even in unrecrystallized surface layer, it is expected that the degree of recovery which has taken place and the substructure formed can have some influence on texture development.

During annealing, manganese in solid solution can be precipitated out in the form of intermetallic particles. This was shown in Figure 11 as conductivity measurements suggest the precipitation of Mn atoms from solid solution and thus results in softening of the overall matrix. However, it should be pointed out that the distribution of finely dispersed secondary phase and coarse primary phase will affect the hardness in the corresponding surface and centre samples. Unpublished work done by the author also showed that the effect of an increasing Mn content in solid solution in this deformation structure is to retard the recrystallization rate of 3004 alloy and hence no recrystallized grains are observed at lower annealing temperature in one hour.

Finally, the implications of the usefulness of this investigation is that recrystallization involves a texture change, so it is clear that it will influence earing control in the final sheet product. For example, if the rolling texture is predominant, then ears will appear at 45° to the rolling direction of the sheet. These are undesirable because metal is wasted and an additional operation is required to remove them from the pressed articles in production. The walls of the extruded products may also be weakened excessively in places. In addition, it may also lead to production problems due to difficulties in ejecting products after a pressing operation. However, the occurrence of recrystallization during hot rolling will reduce the tendency to form the 45° earing problems because of the introduction of a very strong cube texture component into the material by recrystallization and grain growth. Therefore, by careful controlling the rolling and annealing schedules in the processing route, the problems of earing in the can stock can be minimized. In addition, material parameters such as grain size, shape and texture could also be optimized.

Conclusions

The conclusions that can be drawn from this investigation are as follows:

1) There exist a correlation between texture development and driving force for recrystallization.

2) Strength of the cube texture component and the rate of recrystallization increases as the rolling temperature, annealing time and pct reduction increases. However, the rate of recrystallization initially increases then followed by a decreases as annealing time increases.

3) Surface samples showed higher cube texture than the corresponding centre samples. The recrystallization texture was found to consist of a cube texture component, rolling texture component and random texture component.

4) After annealing, recrystallized surface layer with a cube texture and a unrecrystallized core with a rolling texture has developed and the degree of recrystallization depend on the internal strain energy available.

5) The distribution of intermetallic particles has some effect on texture development.

6) The distribution of primary and secondary precipitates have an effect on surface and centre hardness. Higher density of fine, densely concentrated precipitates is harder than those consisting of mostly coarse primary intermetallic particles.

References

[1] U. Koster, *Metal Sci.*, 8, 151 (1974).
[2] J.E. Bailey, *Phil. Mag.*, 5, 833 (1960).

Acknowledgement

The author would like to thank Comalco Research Centre and Royal Melbourne Institute of Technology for the provision of laboratory facilities and the supply of materials.

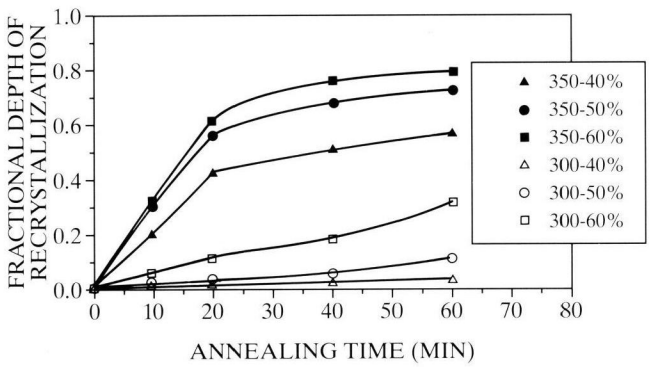

Fig. 1:
Effect of annealing time on the fractional depth of recrystallization at various temperature and pct deformation. No recrystallized grains were observed for samples annealed at 250 and 280 °C at all rolling reductions.

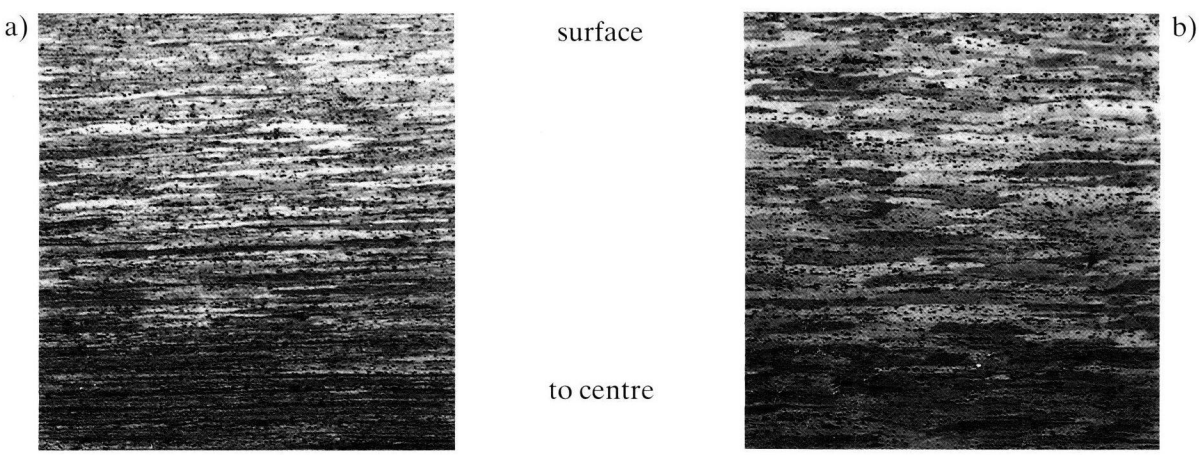

Fig. 2:
Typical microstructures of samples quenched 15 sec on exit from warm mill. (50×) (a) 60% reduction, 350 °C; (b) 40% reduction, 300 °C.

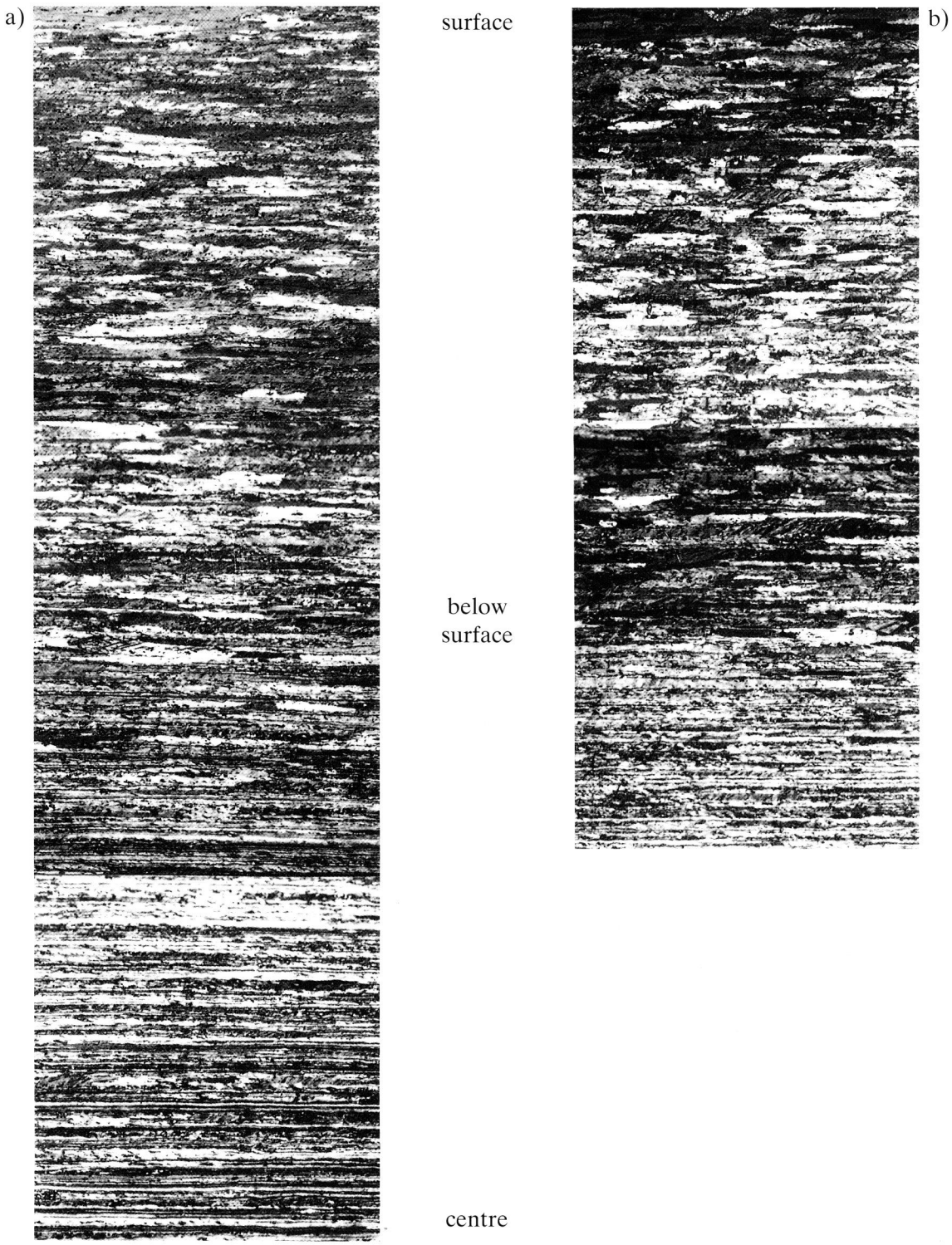

Fig. 3:
Typical microstructures of samples observed after annealing at 300 °C for (a) 20 min., 40% reduction and (b) 60 min., 40% reduction (50×).

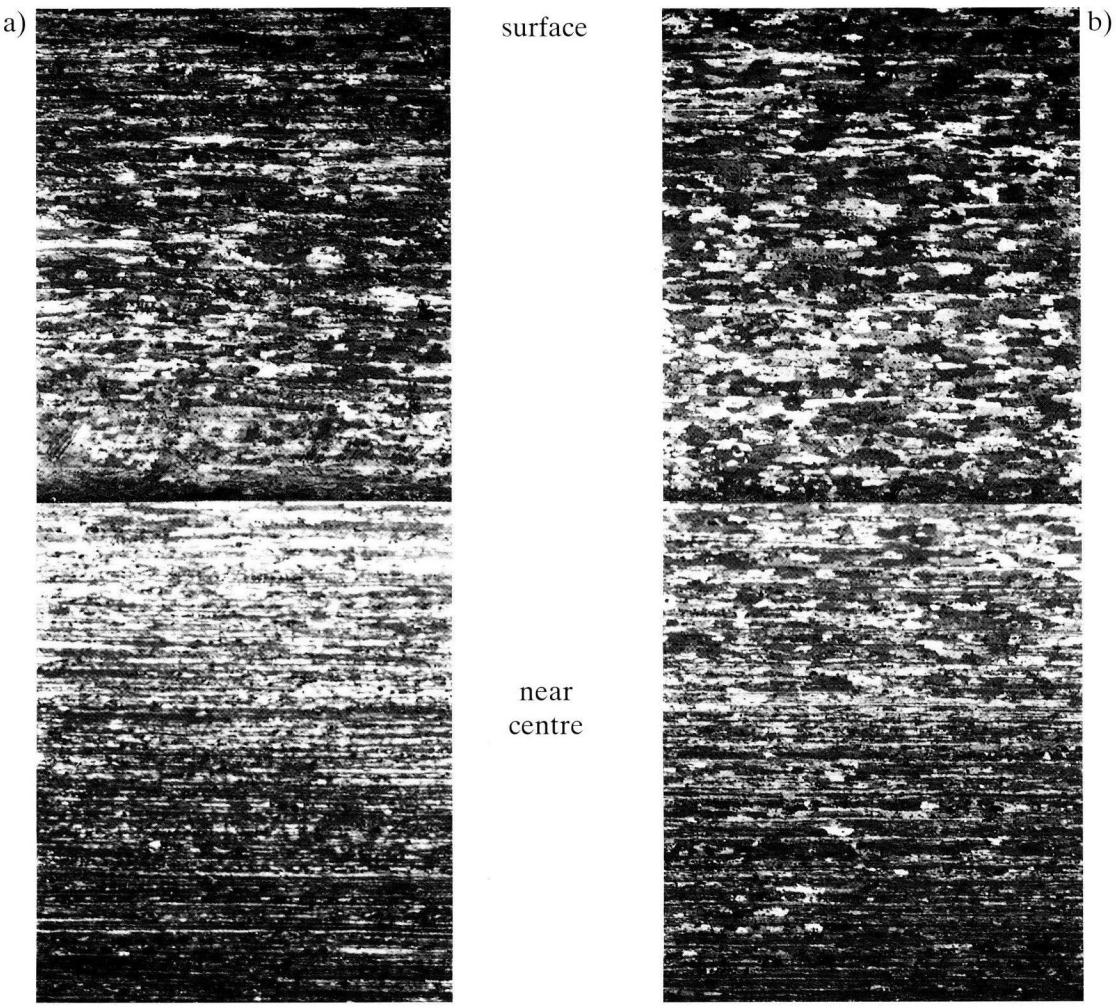

Fig. 4:
Typical microstructures of samples observed after annealing at 300 °C for (a) 20 min., 60% reduction and (b) 60 min., 60% reduction (50×).

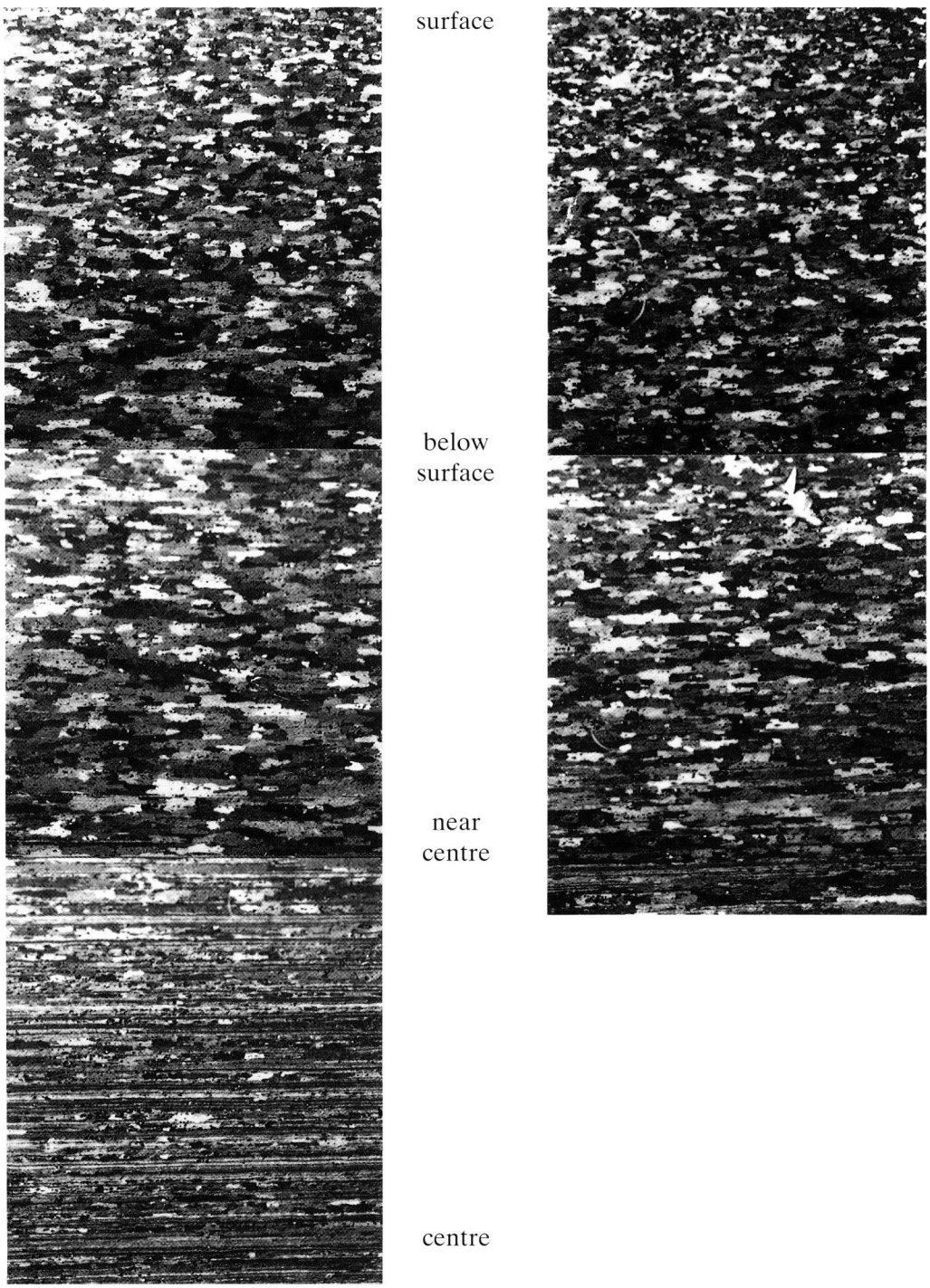

Fig. 5:
Typical microstructures of samples observed after annealing at 350 °C for (a) 20 min., 60% reduction and (b) 60 min., 60% reduction (50×).

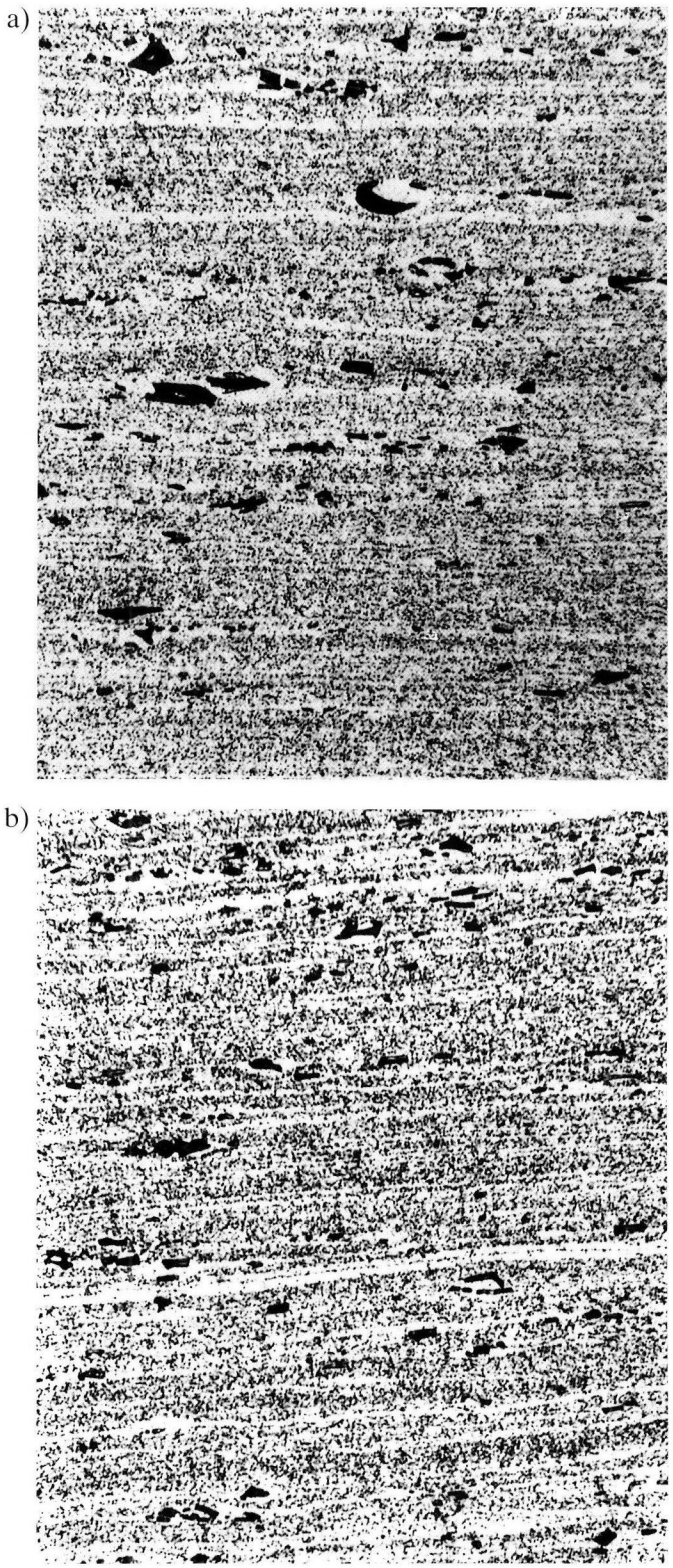

Fig. 6:
Distribution of second-phase particles in hot rolled plate and annealed for 60 min (400×). (Etched by Kroll's Reagent).

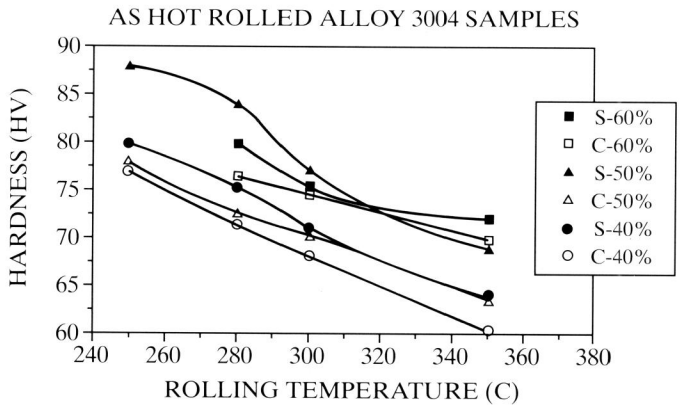

Fig. 7:
Plot of centre (C) and surface (S) hardness versus rolling temperature.

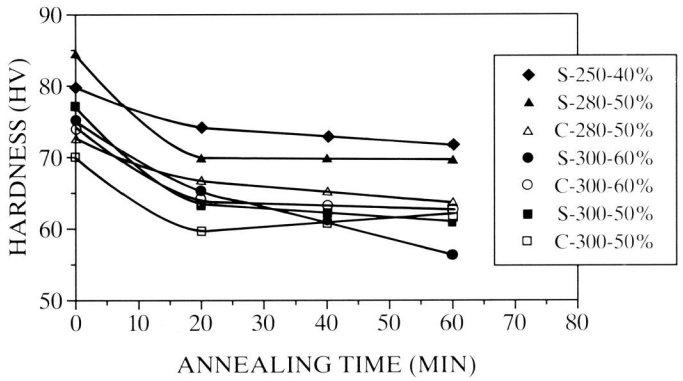

Fig. 8:
Plot of centre (C) and surface (S) hardness versus annealing time for samples soaked at various temperatures.

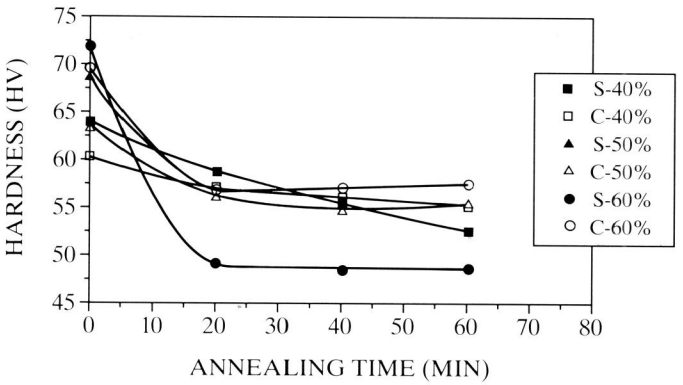

Fig. 9:
Plot of centre (C) and surface (S) hardness versus annealing time for samples soaked at 350 °C.

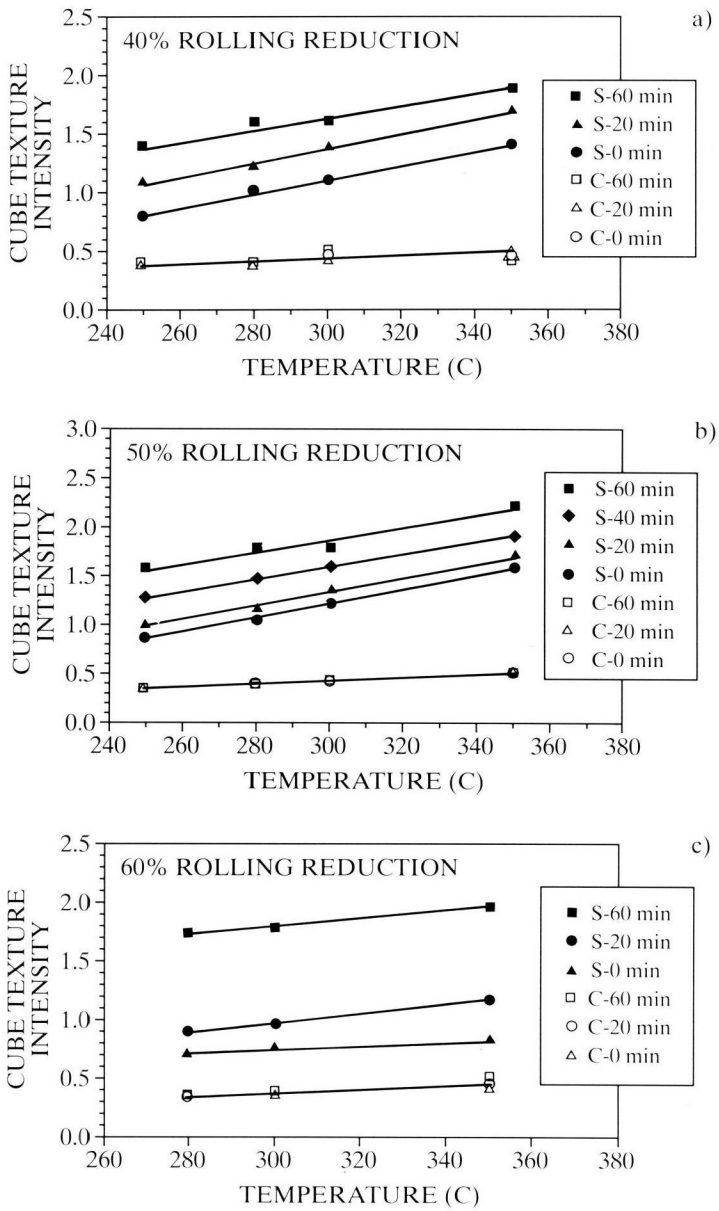

Fig. 10:
Relative cube texture intensity to powder sample versus temperature of as-hot rolled and annealed samples (S = surface. C = centre).

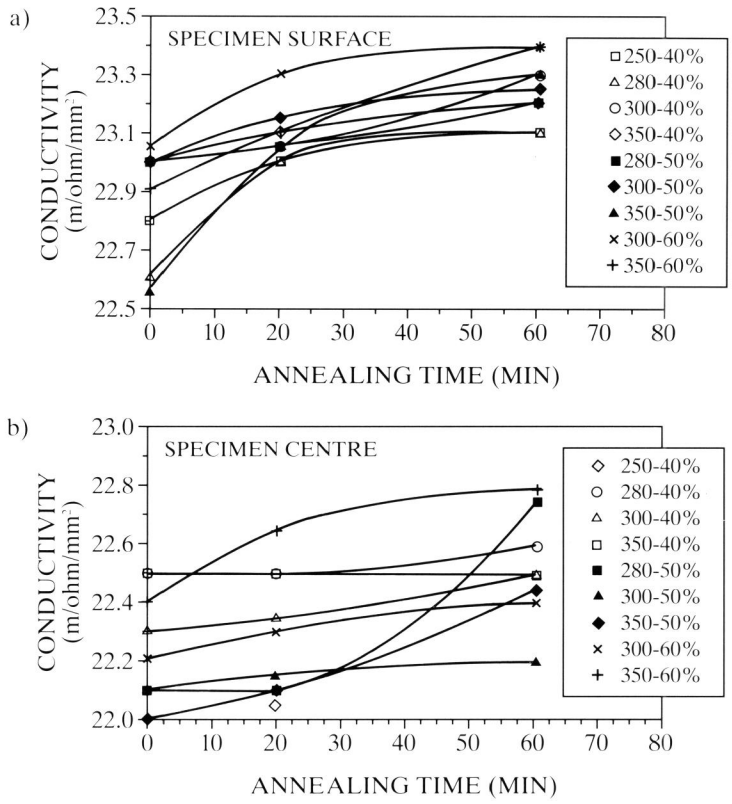

Fig. 11:
Change of electrical conductivity during annealing at various temperature and rolling reduction.
(a) specimen surface; (b) specimen centre.